DOI: 10.1111/cgf.13589

COMPUTER GRAPHICS *forum*
Volume 00 (2018), number 0 pp. 1–16

Incremental Labelling of Voronoi Vertices for Shape Reconstruction

J. Peethambaran[1,2], A.D. Parakkat[1], A. Tagliasacchi[3], R. Wang[4] and R. Muthuganapathy[1]

[1]Department of Engineering Design, Indian Institute of Technology, Madras, India
{jijupnair2000, adp.upasana, emry01}@gmail.com
[2]Department of Mathematics and Computing Science, Saint Mary's University, Halifax, Nova Scotia, Canada
[3]Department of Computer Science, University of Victoria, Victoria, British Columbia, Canada
andrea.tagliasacchi@siggraph.org
[4]Schulich School of Engineering, University of Calgary, Calgary, Alberta, Canada
ruiswang@ucalgary.ca

Abstract

We present an incremental Voronoi vertex labelling algorithm for approximating contours, medial axes and dominant points (high curvature points) from 2D point sets. Though there exist many number of algorithms for reconstructing curves, medial axes or dominant points, a unified framework capable of approximating all the three in one place from points is missing in the literature. Our algorithm estimates the normals at each sample point through poles (farthest Voronoi vertices of a sample point) and uses the estimated normals and the corresponding tangents to determine the spatial locations (inner or outer) of the Voronoi vertices with respect to the original curve. The vertex classification helps to construct a piece-wise linear approximation to the object boundary. We provide a theoretical analysis of the algorithm for points non-uniformly (ϵ-sampling) sampled from simple, closed, concave and smooth curves. The proposed framework has been thoroughly evaluated for its usefulness using various test data. Results indicate that even sparsely and non-uniformly sampled curves with outliers or collection of curves are faithfully reconstructed by the proposed algorithm.

Keywords: curves and surfaces, modelling, computational geometry, geometric modelling

ACM CCS: •*Computing methodologies* → *Computer graphics; Shape analysis*; •*Theory of computation* → *Computational geometry*

1. Introduction

Recovering shape representations of an object from its boundary samples is a fundamental yet challenging problem in a number of fields such as computer graphics, computer vision, computational geometry, photogrammetry and reverse engineering [Lee00, Wan14, MBS16]. A handful of representations such as contours and skeletons, derived from the point set, provide valuable insights into the geometry of the corresponding object. These representative geometric structures play a significant role in shape analysis, especially by boosting the computational performance and reducing the storage requirements. In this work, we develop a multi-purpose Voronoi-based framework for extracting curves, medial axes and dominant points (DPs) from non-uniform and possibly sparse data, sampled from the boundaries of geometric objects. Figure 1 showcases various shape representations extracted by the proposed framework from the points sampled along the contour of a maple leaf. Our shape representations range from highly detailed polygonal curves (Figure 1c) that span the input points to DPs driven, coarse polygonal approximations (Figure 1e) that achieve high-level of data compression. Further, it also approximates medial axes (Figure 1d) of the object from its input samples.

Any simple closed curve divides the plane into a bounded and unbounded region. Voronoi vertices in the unbounded region can be labelled as *outer,* while Voronoi vertices in the bounded region can be labelled as *inner*. The labelling can give reasonable cues about various geometric structures representing the original curve. For instance, a Voronoi edge connecting *inner* and *outer* intersects the original curve. Consequently, its dual Delaunay edge can be used as a linear approximation to the corresponding curve portion. Similarly, all the Voronoi vertices lying in the bounded region approximates the interior medial axis (MA), which can be captured via the corresponding dual Delaunay edges. While these

Figure 1: *Shape representations generated by the proposed framework from non-uniform samples of maple leaf boundary. (a) Representative image, (b) point set (113 points), (c) reconstructed curve, (d) medial axis (interior) and (e) dominant points (DP) shown in blue circles.*

observations are pretty standard in curve reconstruction domain and there have been many attempts to exploit these ideas in curve reconstruction, e.g. power crust [ACK01], a unified framework that handles curves, medial axes and high curvature points (referred to as DPs) is surprisingly missing in the literature.

We introduce a simple incremental Voronoi vertex labelling algorithm to extract these shape representations from points sampled from simple closed curves. Our algorithm heuristically computes the poles at each input sample, where the poles estimate the normals at samples [DW01]. Then, it uses these estimated normals and tangents at sample points along with the Voronoi branching pattern for the vertex classification and subsequently construct a piece-wise linear approximation to the boundary and the interior MA of the original curve. Extreme curvature portions induce specific labelling patterns of the Voronoi diagram (VD) and these labelling patterns are utilized to identify DPs on the input curve. A theoretical evaluation of the incremental labelling algorithm for smooth curves is provided under ϵ-sampling model [ABE98] and we demonstrate the practical potentials of the algorithm via several experiments and comparison with the state-of-the-arts.

2. Related Work

In this section, we briefly review the existing literature on curve reconstruction, MA extraction and DP identification in 2D.

2.1. Curve reconstruction

Over the past few decades, a number of approaches have been proposed for curve reconstruction. Curve reconstruction deals with the task of constructing a polygonal chain faithful to the original curve from its sample data. Most often, input data, acquired through sensors or extracted from images, consist of noise or outliers. These defect-laden data often pose a great challenge to the curve reconstruction problem. A few methods [Lee00, Wan14, CFG*05, dGCSAD11] can deal with the reconstruction of curves from noisy input data. However, most of the Delaunay/Voronoi-based reconstruction techniques interpolate the input data and consequently are less tolerant to noise.

Curve reconstruction from an arbitrary data, insufficiently sampled from an unknown original curve, is highly infeasible [ABE98]. A few conditions on the sampling are needed to guarantee a faithful reconstruction of the original curve. Under uniform sampling, where the adjacent points are sampled at a distance less than a threshold value, many algorithms such as α-shape [EKS83] and r-regular shapes [Att98] are known to work with reasonable accuracy. However, uniform sampling condition leads to dense sampling all over the curve, including the areas where a sparse sampling would be sufficient.

To capture the local level of details at each point sampled on a smooth curve, highly detailed portions of the curve demand a dense sampling, whereas the portions that encapsulate less details can be less densely sampled. Based on this observation, Amenta, Bern and Eppstein [ABE98] introduced a non-uniform sampling model called ϵ-sampling (Definition 4), where the sampling density varies with the *local feature size* on the curve. Using the idea of ϵ-sampling, they proposed *crust* algorithm which guarantees to construct a piecewise linear approximation to a smooth curve, for certain $\epsilon < 0.252$. Subsequently, a few variants of crust such as nearest neighbour crust [DK99] and a locally defined crust [Gol99] were proposed. It is remarkable that nearest neighbour crust algorithm, though very simple in conception, improved the value of ϵ to 0.333 from 0.252. Later, conservative crust [DMR00], that reconstructs a collection of open and closed smooth curves, was described. Compared to the previous crust algorithms, conservative crust showed better resistance towards noise and outliers at the expense of a parameter tuning.

Crust and its variants fail in theory as well as in practice, for curves with sharp corners [DW02]. Using a different sampling condition for corner areas, Giesen [Gie99] showed that the travelling salesman tour of a point set densely sampled from a single closed curve Σ (possibly with corners) represents the correct reconstruction of Σ. In his work, the tangents (left and right) at any point on the curve must make a non-zero angle for a guaranteed reconstruction. By formulating travelling salesman problem in terms of a linear program and applying the ellipsoid method, Althaus and Mehlhorn [AM01] showed that the travelling salesman tour can be found in polynomial time for curve reconstruction. Dey and wenger [DW01] described a heuristic called *gathan* that handles corners and endpoints and subsequently, in [DW02], they extended 'gathan' to reconstruct a collection of piece-wise smooth closed curves with provable guarantee. Funke and Ramos [FR01] introduced the concept of angular sampling where the angle determined by any edge (p_1, p_2) in the correct reconstruction and any other sample point p_3 is upper bounded by a constant, θ_{angle}. Under this sampling, they

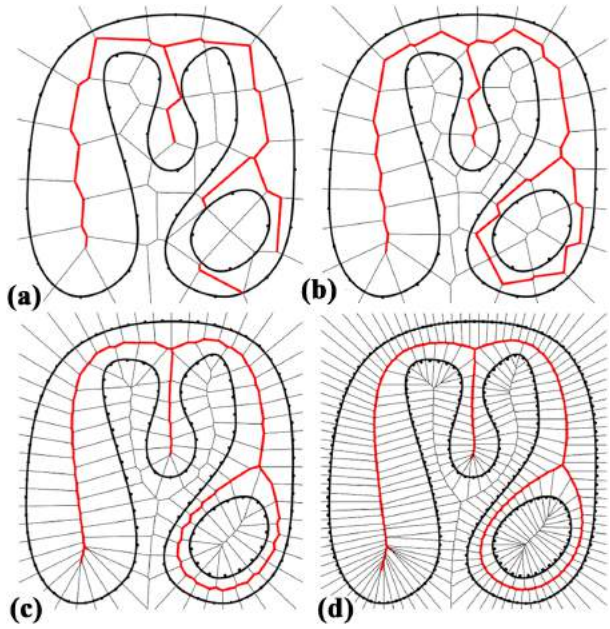

Figure 2: *Relation between medial axis and Voronoi diagram. As the sampling rate increases, the Voronoi vertices converge to the medial axis. [Image courtesy: [TDS*16]]*

proposed an algorithm based on empty β-balls to handle a collection of curves with corners and end points.

Despite two decades of research, curve reconstruction is still an active problem among the computational geometry and computer graphics research communities. Recent research trends target aspects such as improved sampling conditions [OMW16], reconstructing from fewer number of samples and curves with sharp corners [OM13], reconstruction from unstructured and noisy point cloud [OW18], unified frameworks for curve and shape reconstruction [MPM15], and applications of curve reconstruction to hand drawn sketches [PM16]. The proposed algorithm is a modified extension of the water flow-based labelling algorithm proposed in [PPM15]. Compared to [PPM15], we have described the labelling framework in a formal setting with an additional technique for DP detection and the algorithm has been validated using extensive experiments.

2.2. Medial axis approximation

The *medial axis* of a curve $\mathcal{C}$ is defined as closure of the set of points in the plane which have two or more closest points in $\mathcal{C}$ [ABE98]. It is a powerful shape descriptor, widely used in shape analysis and feature extraction [FEC02]. Approximating the MA from the VD of points sampled along the boundary of objects has been addressed in [Gol99, FEC02, BA92, Bra94, GMP07a, ACK01, AK01, AM97]. Brandt and Algazi [BA92, Bra94] showed the relationship between the MA of a continuous regular shape and the VD of the points sampled along the border of the shape. Later, Fabbri *et al.* [FEC02] proved that all Voronoi vertices are also MA points (refer to Figure 2). More recent techniques generate the MA by minimizing the quadric error [LWS*15] or one-sided Hausdorff distance [ZSC*14] between the input shapes and the medial spheres. The research on MA computation from defect laden point clouds is still active, e.g. Zhong and Cheng [ZC18] proposed an algorithm to construct compact MA from noisy and or occluded point clouds via approximating the signed distance function by a sparse optimization technique. A recent survey on medial skeletons providing formal definitions, a taxonomy of 3D skeletons and 3D shape skeletonization, can be found in [TDS*16]. In our method, the set of *inner* Voronoi vertices obtained as a result of Voronoi vertex labelling approximates the interior MA of $\mathcal{C}$ (as shown in Figure 1d). We observe that our MA approximation is related to the union of inner Voronoi balls centred at Voronoi vertices. Hence, the theory developed in [GMP07a] is equally applicable to the proposed MA extraction.

2.3. Dominant point detection

In [Att54], Attneave observes that 'the information on a curve is concentrated at points where the curve changes direction most rapidly'. This seminal observation led to many other subsequent approaches for finding the curvature extrema on the boundary of a planar object, see Figure 1(e). These extrema, commonly known as *dominant points (DPs)*, can suitably describe the curve for both visual perception and recognition [Wu02].

Research on DPs primarily focused on highly compressed linear polygons (obtained through DPs) that best approximate the input shape. In general, polygonal approximation techniques based on DPs fall in one of the three categories: sequential approaches, split-and-merge approaches and heuristic approaches [Mas08]. Sequential approaches employ ideas such as longest possible line segments with minimum possible errors [RR93], region of support of each point [TC89, MS03] or mini-max technique [KD82]. Split-and-merge approaches mainly differ in the manner that the curve has been split and this splitting procedure ranges from boundary segmentation [Ram72] through cornerity index [GDN04] to slope difference [HAA94]. Heuristic approaches for polygonal approximations mainly use either dynamic programming [Dun86, Sat92] or genetic algorithms [HS99, PNK98, YIN99]. Existing methods, mostly proposed in pattern recognition domain, target at polygonal approximation of digital curves. Conversely, we adopt a computational geometry approach to extract high curvature points from non-uniform boundary samples of known/unknown geometric objects.

3. Algorithm

We begin by defining the fundamental geometric structure, i.e. the VD, upon which the entire algorithm is designed, and introduce a few terminology relevant for discussing the incremental labelling algorithm.

3.1. Definitions and notations

Let $\mathcal{C}$ be a smooth, simple and closed curve (1-manifold) embedded in $\mathbb{R}^2$. Let P be a set of n points sampled from $\mathcal{C}$ and $Conv(P)$

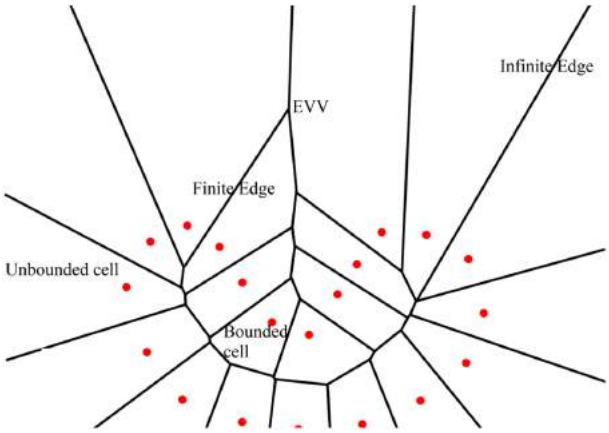

Figure 3: *Voronoi diagram of a set of curve samples.*

denotes the convex hull of S. Further, $d(p,q) = \|p - q\|$ denotes the Euclidean distance between two points $p, q \in P$.

Definition 1. *Voronoi cell (V_p) [O'R98]:*

A Voronoi cell of $p \in P$ is the set of all points in the plane that are closer (or at least equidistant) to p than any other point in P:

$$V_p = \{x \in \mathbb{R}^2 \mid d(p,x) \leq d(q,x), \text{ where } p \neq q, \forall q \in P\}$$

Voronoi diagram of P, denoted by $Vor(P)$, is the subdivision of the plane into Voronoi cells with one cell V_p for each point $p \in P$. The locus of points on the plane that are equidistant from exactly two points, p and q, is called a *Voronoi bisector* and a point that is equidistant to three or more points in P is called a *Voronoi vertex*. A simply connected subset of Voronoi bisectors is called a *Voronoi edge*. The VD consists of bounded and unbounded Voronoi cells. A cell V_p is unbounded if the sample p lies on the convex hull of P. Unbounded Voronoi cells induce what is called as infinite edges, whose one vertex lies at infinity. All Voronoi vertices except the vertex at infinity are *finite*. We use the term *extreme Voronoi vertex (EVV)* to refer to the finite Voronoi vertex of an infinite Voronoi edge (refer to Figure 3). Observation 1 states a property of EVV, which is exploited in the proposed incremental labelling.

Observation 1. *An extreme Voronoi vertex of a Voronoi diagram always belongs to two unbounded and one bounded Voronoi cells.*

Definition 2. *Delaunay triangulation ($Del(P)$) [O'R98]:*

The straight line dual graph of $Vor(P)$ results in a planar triangulation called as Delaunay triangulation of P, $Del(P)$.

Pseudo-concavity. We assume that $\mathcal{C}$ is positively oriented (counter clockwise) closed, smooth and simple curve in 2D (refer to Figure 4a). A *medial ball* $B(c,r)$, centred at $c \in$ MA of $\mathcal{C}$ with radius r, is a maximal ball whose interior contains no points of $\mathcal{C}$ [ABE98]. Let E be the set of all open connected regions of $Conv(\mathcal{C}) \setminus \mathcal{C}$. Each region given by the closure $\overline{E}$ is defined as a *pseudo-concave region* ($\mathcal{PC}_R$) of $\mathcal{C}$ (Figure 4a). The portion of $\mathcal{C}$ in each $\mathcal{PC}_R$ is called *pseudo-concavity*, denoted by $\mathcal{PC}$. The edges

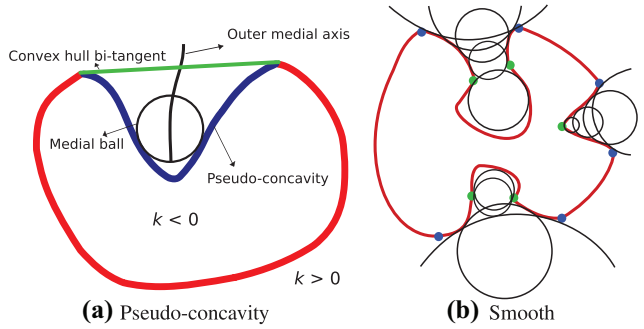

Figure 4: *Illustration of pseudo-concavity and bi-tangent neighbourhood portions of a simple closed curve in 2D. In (b), pseudo-concave portions between blue and green points represent the bi-tangent neighbourhood convergent (BNC) portions.*

of $Conv(\mathcal{C})$ in each *pseudo-concave region* are called convex hull bi-tangents (BT_{cvx}). Every pseudo-concavity is capped by exactly one convex hull bi-tangent.

The curve $\mathcal{C}$ is closed and concave and therefore consists of convex and concave portions. We consider two sets, a concave set $\mathcal{C}_{ccv}$ consisting of all the pseudo-concavities of $\mathcal{C}$ and a pseudo-convex set $\mathcal{C}_{cvx}$, containing all the portions of $\mathcal{C}$ except $\mathcal{C}_{ccv}$, i.e. $\mathcal{C} \setminus \mathcal{C}_{ccv}$. Note that the intersection of $\mathcal{C}_{cvx}$ and $\mathcal{C}_{ccv}$ consists of bi-tangent points belonging to $Conv(\mathcal{C})$.

Bi-tangent neighbourhoods. Based on the radii of medial balls [ABE98], we characterize a property of the curve portions of $\mathcal{C}$, lying in the vicinity of the bi-tangents. The medial balls of a pseudo-concavity, $\mathcal{C}$, tend to increase or decrease as it traverses through the outer MA lying in $\mathcal{C}_R$. The region in $\mathcal{PC}_R$, where the medial ball monotonically increases or decreases, is defined as a *rolling interval* of the medial ball.

Definition 3. ***Bi-tangent neighbourhood convergence (BNC):***

Bi-tangent neighbourhoods of a pseudo-concavity, $\mathcal{C}$, is said to be convergent, if the radius of the medial ball decreases monotonically in the first rolling interval, as it rolls along the outer medial axis of $\mathcal{C}$ from the convex hull bi-tangent end to its interior.

In the case of smooth, concave and closed curves, viewed from the convex hull bi-tangent end, one can observe that the curves leading to the interior of $\mathcal{C}$ in the neighbourhood of convex hull bi-tangent appear to be always converging. Figure 4(b) shows an example of BNC concave curve with a few pseudo-concavities, each having a rolling interval [the curve portions between the bi-tangent points (blue coloured) and the red points] where the radii of its medial ball decrease as it rolls along the corresponding outer MA from the convex hull bi-tangent.

Sampling condition. Most of the reconstruction algorithms impose certain criteria on the sampling in order to provide theoretical guarantees on the reconstruction. A widely used sampling criterion is ϵ-sampling [ABE98], where the sample spacing along the curve is determined by the local feature size (lfs) of the input curve (lfs of samples in particular). *Local feature size* at a point p on $\mathcal{C}$, $LFS(p)$,

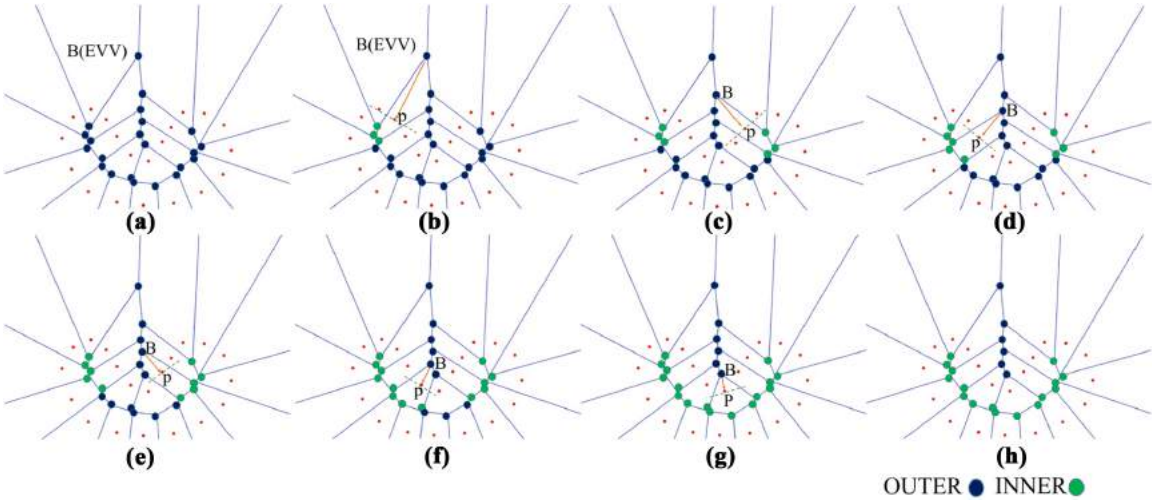

Figure 5: *Illustration of incremental labelling in a concave portion of a closed planar curve. In the figure, red dots constitute the input points sampled from the curve, green and dark blue vertices, respectively, represent the inner and outer (w.r.t original curve) Voronoi vertices in the classification. Incremental labelling starts from an EVV and progresses towards the high curvature points in the concavity.*

is the distance from p to the closest point on the MA of $\mathcal{C}$. A formal definition of ϵ-sampling follows:

Definition 4. *ϵ-sampling [ABE98]: For a constant $\epsilon > 0$, $\mathcal{C}$ is said to be ϵ-sampled by a finite set of samples P, if $\forall p \in \mathcal{C}, \exists s \in P$ such that $\|p - s\| \leq \epsilon LFS(p)$.*

3.2. Incremental labelling in pseudo-concavities

In any closed curve, concave components pose great challenges for reconstruction. Hence, we explain the labelling procedure by taking a concave portion of a simple closed curve. Labelling for convex curves is rather simple and direct. All the Voronoi vertices are initially labelled as *outer* (illustrated using the dark blue points in Figure 5a). Incremental labelling in a pseudo-concavity starts with an EVV. Under dense sampling, each pseudo-concavity has at least one EVV lying outside the $Conv(P)$ as established in Lemma 3.1. An EVV has exactly two unbounded Voronoi cells due to the infinite edge and one bounded Voronoi cell adjacent to it (OBSERVATION 1). The EVV is paired with the sample of its adjacent bounded cell. Starting from the EVV, the labelling process progresses to any unvisited *outer* Voronoi vertex adjacent to it. A few *outer* Voronoi vertices undergo label transitions from *outer* to *inner* during the incremental labelling process.

Lemma 3.1. *$Vor(P)$, where P is densely sampled (ϵ-sample) from a smooth, closed, pseudo-concave and planar curve $\mathcal{C}$, has at least one finite Voronoi vertex outside $Conv(P)$.*

Proof. Without loss of generality, we consider the bi-tangent neighbourhood convergent portions (Definition 3), $\overset{\frown}{qb}$ and $\overset{\frown}{ap}$ of a pseudo-concavity $\mathcal{C}$, in the counter-clockwise direction of $\mathcal{C}$ (Figure 6a). Let $\bar{xy}$ constitute the convex hull edge capping $\mathcal{C}$ where $x \in P$ and $y \in P$ are either p and/or q or neighbourhood points of p and/or q (refer to Figure 6b). Let $z \in P$ be the sample belonging to either $\overset{\frown}{qb}$ or $\overset{\frown}{ap}$ that is closest to either x or y. Under a dense sampling, an

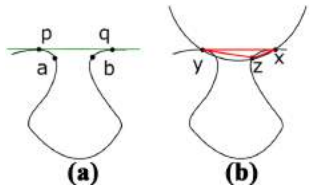

Figure 6: *Illustration of Lemma 3.1.*

empty circle passing through x, y and z is always possible whose circumcentre lies outside $Conv(P)$ (shown in Figure 6b) and hence the lemma. □

The condition that triggers the label transition of a Vorornoi vertex is based on the normal estimation technique proposed in [AB98]. Amenta and Bern [AB98] observed that Voronoi cells of P, where P is ϵ-sampled from a curve, $\mathcal{C}$, tend to elongate in the direction of the normal at each point. In [AB98], the authors define *poles*, which are two EVVs of V_p, for each sample point p. In the case of curves, the reason for which the line passing through p and any of the two poles estimates the normal at p is explained in [DW01].

For a Voronoi cell V_p of a sample point, the outer Voronoi vertex where the labelling process starts represents its source Voronoi vertex (SVV). Each sample p in P has its own Voronoi cell V_p, and hence one of the vertices of V_p subjected to the labelling procedure is guaranteed to be the SVV of p.

Consider a bounded Voronoi cell V_p and its SVV (represented as B_p) along with its owner point p as shown in Figure 7. The line L, orthogonal to $\overrightarrow{B_p, p}$, divides the plane into two half planes designated as $H_1(p)$ and $H_2(p)$. Using the vector, $(B_p - p)$ and L, we present the state transition rule for a Voronoi vertex in our model in Definition 5.

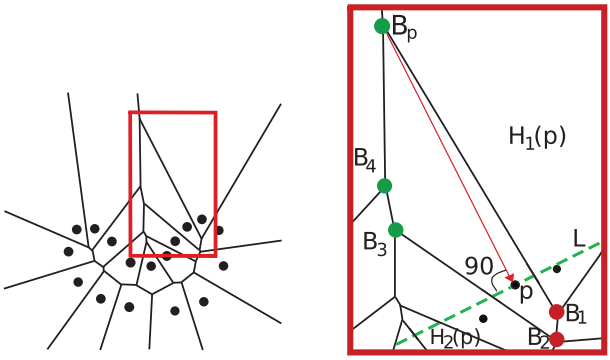

Figure 7: *A bounded Voronoi cell with the normal (red line with arrow) and the tangent (green coloured dashed line) of the sample,* outer *(green points), and* inner *(red points) Voronoi vertices.*

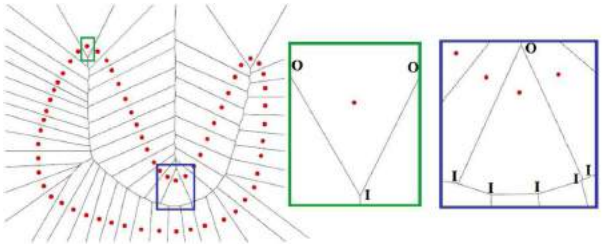

Figure 8: *Different labelling patterns on the Voronoi cells of dominant points. Green and blue boxes depict examples of OIO and IOI patterns, respectively.*

Definition 5. *Label transition rule:*

Let B_i be an outer *Voronoi vertex of a Voronoi cell V_p of a sample point p and B_p be the source Voronoi vertex of V_p, B_i is labelled as* inner *if B_p and B_i lie on either side of L.*

Algorithm 1: IncrementalLabel(B)

Input: Branch Voronoi vertex, B
1 Let p be the unpaired sample in the three Voronoi cells of B;
2 Pair p with B;
3 Apply state transition rule (Definition 5) to B in V_p;
4 **if** *there are no neighboring outer and unvisited vertices for B* **then**
5 | **return**;
6 **end**
7 **else if** *there is one neighboring outer and unvisited vertex for B* **then**
8 | Let B_{new} be the outer neighboring vertex of B;
9 | IncrementalLabel(B_{new});
10 **end**
11 **else**
12 | Let B_{new1} and B_{new2} be the outer neighboring vertices of B;
13 | IncrementalLabel(B_{new1});
14 | IncrementalLabel(B_{new2});
15 **end**

Essentially, the source vertices estimate the poles of the samples as established in Lemma 3.2 and consequently, the vectors, $(B_p - p)$ and L, approximate the normal and tangent at p, respectively. So, all the Voronoi vertices of V_p beyond p when viewed from B_p are labelled as *inner*. The justification is that the Voronoi vertices lying beyond the estimated tangent L of p also lie inside the original curve and hence can be considered as *inner*. The labelling algorithm advances to any neighbouring unvisited outer Voronoi vertices of B_p (Figures 5c–f) and is repeated until there are no neighbouring unvisited outer Voronoi vertices for the current B_p (refer to Figure 5g). The incremental labelling in pseudo-concavities is presented in Algorithm 1. While the first recursive call (line 7 of Algorithm 1) helps to traverse a single Voronoi branching, the second recursive call (lines 11 and 12 of Algorithm 1) helps to traverse the two new Voronoi branchings corresponding to two inner pseudo-concavities. All the Voronoi vertices are visited exactly once during the Incremental_Label() on B_p.

Lemma 3.2. *In $Vor(P)$, where P is ϵ-sampled from a smooth, concave and closed planar curve $\mathcal{C}$, source Voronoi vertex (B_p) of a sample point p represents one of the poles of p.*

Proof. Amenta *et al.* [AB98] have observed that the poles of the VD of a sampling of a smooth curve converge to the MA. Hence, under dense sampling (as ϵ approaches to zero), the positive pole of each sample lies on the exterior MA. The incremental labelling procedure starts with the EVV of a pseudo-concavity and EVV approximates one of the points in the exterior MA. Hence, EVV represents the positive pole of the sample from its bounded Voronoi cell. As the transition rule (Definition 5) restricts the labelling procedure to the pseudo-concave region, i.e. the labelling advances only along the Voronoi vertices from the exterior MA of the pseudo-concave region, all the source Voronoi vertices obtained through such a labelling represent the poles of samples along the pseudo-concave curve portion. □

Algorithm 2: ExtractShapes(P)

Input: Point set P
Output: $curve(P)$
1 Construct $Vor(P)$ and its dual $Del(P)$;
2 Label all the vertices of $Vor(P)$ including the INFINITE vertex to outer;
3 Pair up the samples in unbounded Voronoi cells with INFINITE vertex;
4 Construct a heap priority queue, PQ containing $EVVs$ lying outside the convexh ull of P, sorted in the descending order of their circum radii of the dual Delaunay triangles;
5 **while** *PQ not empty* **do**
6 | B=root(PQ), delete B from PQ;
7 | Incremental_Label(B);
8 **end**
9 Extract the graph, $curve(P) = \{e \mid$ edge $e \in Del(P)$ and $Dual(e)$ has outer and inner vertices$\}$;
10 Extract the graph, $MAT(P) = \{e \mid$ edge $e \in Vor(P)$ and e has either two inner or outer vertices$\}$;
11 **return** *curve(P)*;

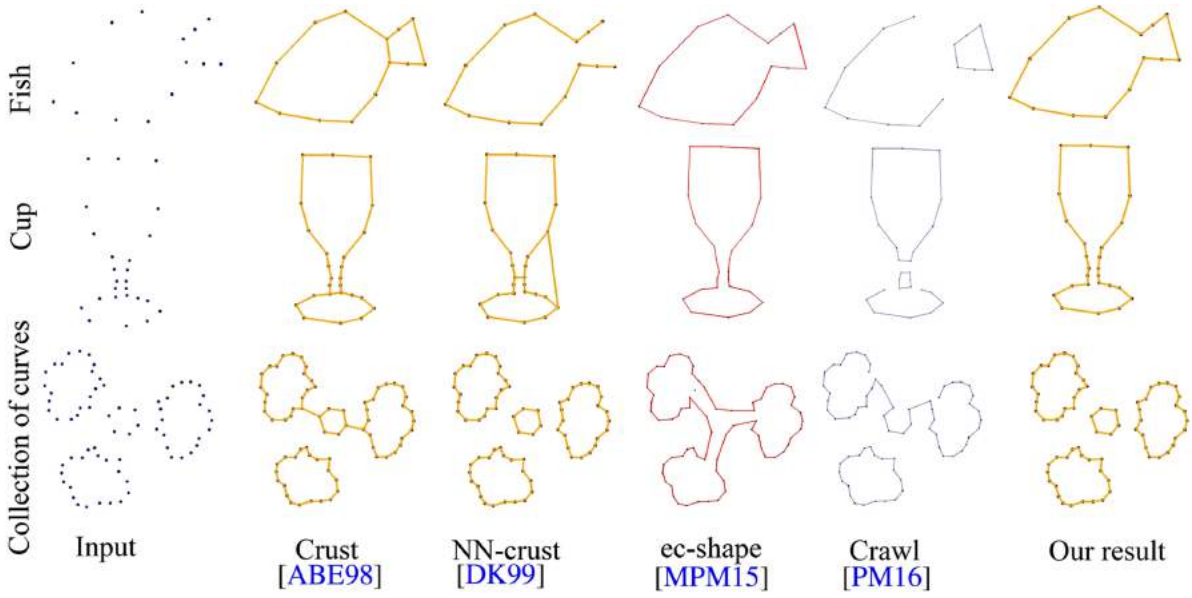

Figure 9: *Reconstruction results of various algorithms on sparse data.*

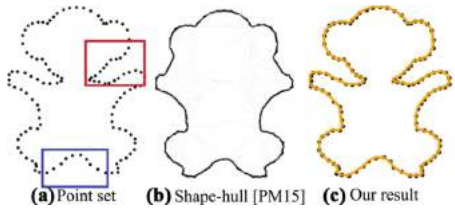

Figure 10: *Reconstruction of monkey point set. In (a), blue box contains a divergent concavity [PM15b] and a red box encapsulates a non-divergent concavity.*

We would like to point out that a similar labelling approach has been adopted in [GMP07b] to compute the MA of the union of inner Voronoi balls. However, the method proposed in [GMP07b] depends on a locally defined crust [Gol99], for the classification of Voronoi vertices. As opposed to this, the Voronoi vertex labelling in our approach is based on an incremental approach and hence in addition to the MA approximation, our method is also capable of reconstructing the boundary of the input sample.

3.3. Curve and medial axes extraction

We assume that no four points are co-circular and hence each finite Voronoi vertex has a degree of 3. A pseudo-code for curve reconstruction is provided in Algorithm 2. It starts with the construction of $Vor(P)$ and its dual $Del(P)$. Each Voronoi vertex structure is equipped with the **label** and **visited** fields to keep track of the vertex label and the visited status during the incremental labelling. All the Voronoi vertices are initialized to *unvisited* in the beginning. Under dense sampling, EVVs of infinite Voronoi edges induced by any pair of adjacent samples from pseudo-convex portions lie inside $Conv(P)$. This is established for ϵ-sampling in Lemma 5.1, see Appendix. For convex portions, the convex hull is a linear approximation to the original curve and hence, these vertices also lie in the interior of the original curve. So, we label all such EVVs as *inner*. All the remaining Voronoi vertices

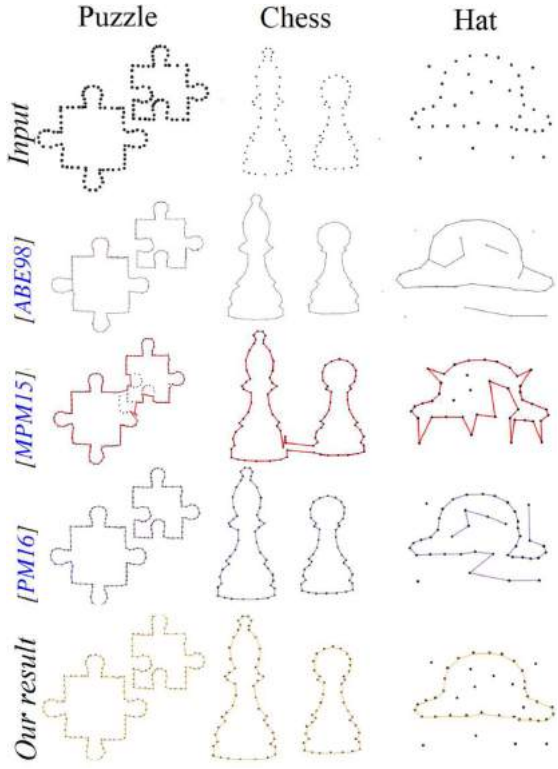

Figure 11: *Reconstruction from collection of curves and curves in the presence of outliers.*

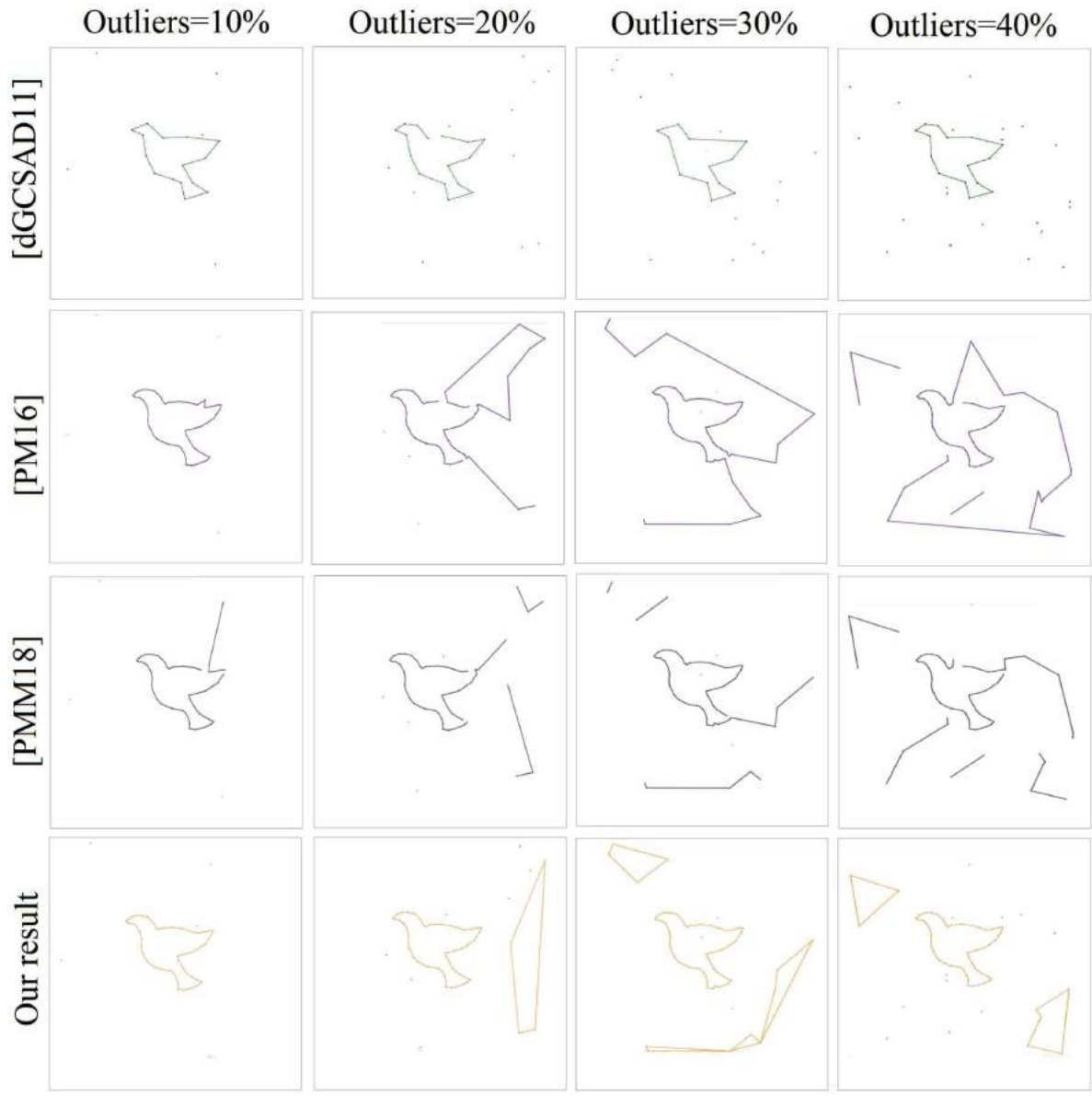

Figure 12: Outlier experiment: *All the stages of outlier injection, dove shape reconstructed by the proposed algorithm, preserve fine details as compared to a simplified reconstruction by deGoes et al. [dGCSAD11] and the reconstruction with curve artefacts in [PM16] and [PMM18]. Outliers were generated using the software by deGoes et al. [dGCSAD11].*

are labelled *outer* at the start of the incremental labelling process. In the next step, a heap-based priority queue, PQ of all the *outer* EVVs, is created, where the EVVs are sorted in the descending order of the circumradii of the corresponding dual Delaunay triangles. In each iteration, the algorithm picks the root element from PQ and applies the vertex labelling procedure given in Algorithm 1.

Once the incremental labelling has been applied to all the EVVs in PQ, it extracts the curve and MAT from $Del(P)$ by employing Dual() function which gives the dual Delaunay edge of a Voronoi edge. The algorithm has been designed to address closed curves, and hence, we have avoided few conditions that may arise in the cases of open curves. Nevertheless, these additional conditions may be incorporated to extend the practical potentials of the proposed algorithm.

The number of Voronoi vertices is linear in terms of the point set size, n. Since each Voronoi vertex is visited exactly once in the IncrementalLabel() procedure, loop of Algorithm 2 costs only $O(n)$. Other operations such as label initialization, and curve and MAT extractions take linear time. As the number of EVVs is very low compared to the input samples, PQ creation and heapify costs are negligible. So, the worst case time complexity of the algorithm

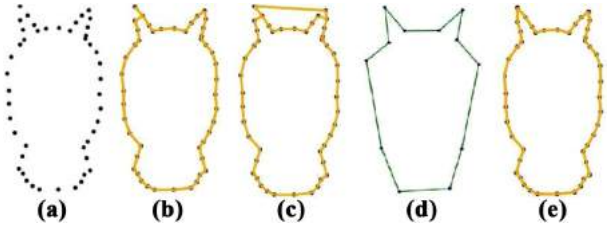

Figure 13: *Reconstruction of oni data. (a) Point set, (b) crust [ABE98], (c) nearest neighbour crust [DK99], (d) result of [dGCSAD11], and (e) our result.*

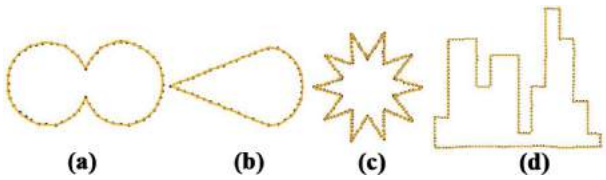

Figure 14: *Results of curves with sharp features.*

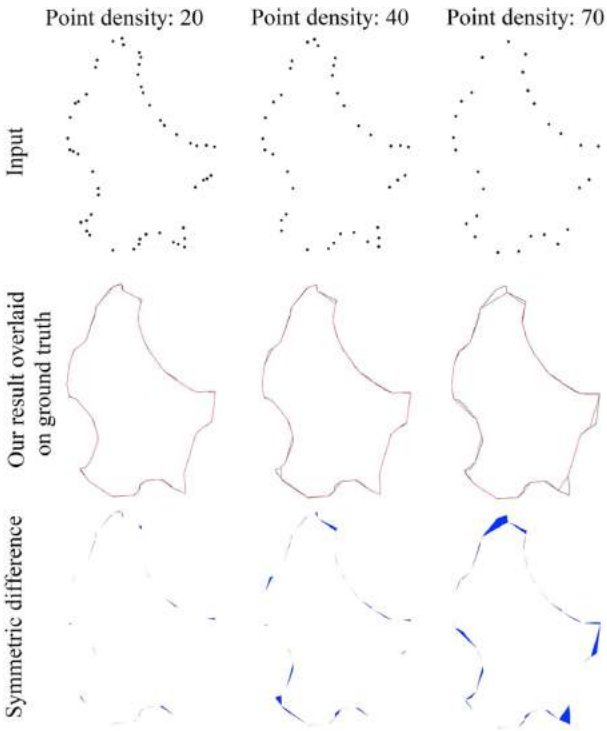

Figure 15: *Illustration of L^2-error metric.*

is $O(n \log n + k \log k)$, where $k = \#EVVs$, and is mainly incurred due to the computation of VD.

3.4. Dominant points detection

The labelled VD obtained through the incremental labelling (Algorithm 1) can be further used to identify the points with high

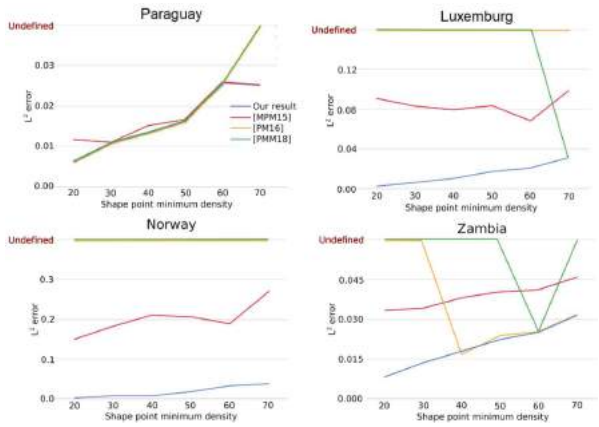

Figure 16: *Variation in the accuracy of reconstruction (quantified in terms of L^2-error metric) with the changing sample density of various inputs.*

curvature values (or DPs). We observe that a few of the vertices from the Voronoi cells of such points conform to interesting labelling patterns. The patterns are formed out of the labels of three consecutive Voronoi vertices along the Voronoi cell boundary, where each pattern consists of vertices with same labels at either side and a centre vertex with a different label as shown in Figure 8. Since the Voronoi vertices are labelled either as *inner* or *outer*, we have only two such labelling sequences referred to as *IOI* and *OIO* patterns (here, *inner* is abbreviated as *I* and *outer* is abbreviated as *O*). Under reasonably dense sampling along the curvature portions, which is often guaranteed in non-uniform sampling such as ϵ-sampling, the Voronoi cells of points from curvature extremes tend to have either *IOI* or *OIO* patterns on their Voronoi cells. This observation leads to a simple and immediate extraction scheme for DPs.

Input points with *IOI* or *OIO* patterns on their Voronoi cells are extracted as DPs subjected to one more constraint, which filters out most of the false positives. We use a constraint similar to the state transition rule (Definition 5). Let c, t_1, t_2 be the central and the terminal vertices of an identified pattern (*IOI* or *OIO*) over the Voronoi cell of an input point p, respectively. We consider the line L going through p and orthogonal to the vector $\overrightarrow{cp}$. The pattern and consequently the point is a qualified DP, if the central vertex c and the terminal vertices lie on either side of L. The DP extraction consists of a linear traversal over the Voronoi cells, a constant circular traversal over the vertices of a cell for identifying the discussed patterns and a constant time location check for the pattern vertices. Hence, the time complexity of DP extraction is $O(n \log n)$, mainly due to VD computation.

4. Experimental Results

We implemented our algorithm in C++ using computational geometry algorithms library (CGAL). To evaluate the performance of our approach, we tested it on points sampled randomly from the contours of silhouettes from MPEG 7 CE Shape-1 Part B and aim@shape repositories. A few data sets were generated from the corresponding images using mesecina software [MGP07]. We

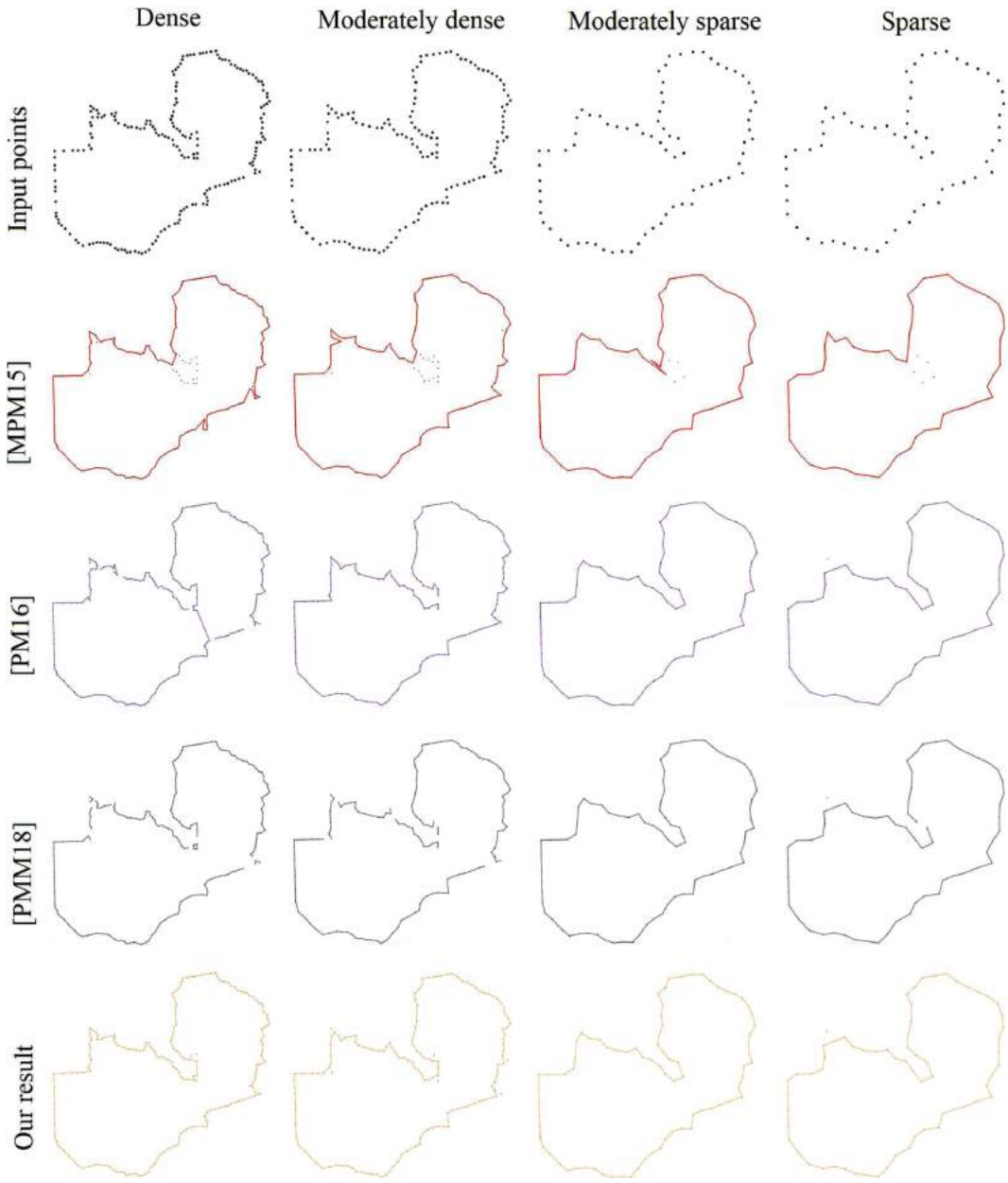

Figure 17: *A qualitative comparison of the curve reconstruction algorithms for Zambia point set with varying sampling densities. See Figure 16(d) for the quantitative results.*

compared our algorithm with other Delaunay/Voronoi-based algorithms such as crust [ABE98], nearest neighbour crust [DK99], ec-shape [MPM15], shape-hull [PM15b] and the recent algorithms in [PM16] and [PMM18]. We also evaluate our method using simplification algorithms such as optimal transport-based algorithm [dGCSAD11].

Reconstruction from sparse data. Sparse data represent a major challenge to any type of curve reconstruction algorithm, especially, when geometrical or topological information of the original curve is unknown. In practice, the proposed algorithm performed well for a variety of sparse and non-uniform input data as shown in Figure 9. For shapes such as the fish and the cup, the results generated by our algorithm and ec-shape [MPM15] are noticeably better as compared to the results of Delaunay-based algorithms. Intuitively, the normal and tangent-based vertex classification allows for a reasonably correct reconstruction even when the sampling is sparse.

In [PM15b], the authors propose shape-hull algorithm that reconstructs divergent concave curves and surfaces from their non-uniform samples. We would like to point out that our algorithms

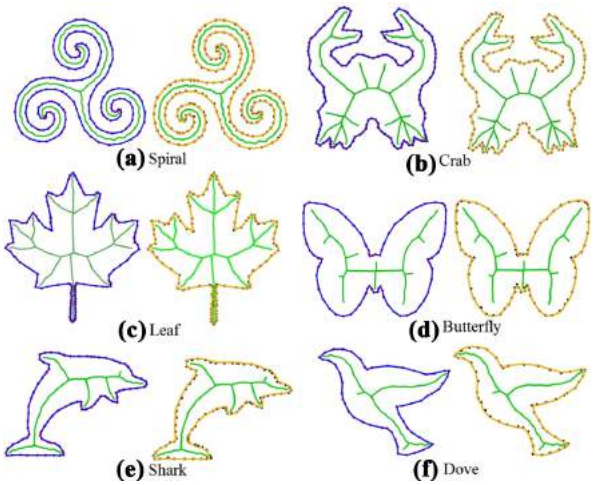

Figure 18: Medial Axes Gallery*: MAT generated for various non-uniformly sampled data by local crust [Gol99](column 1) and our algorithm (column 2).*

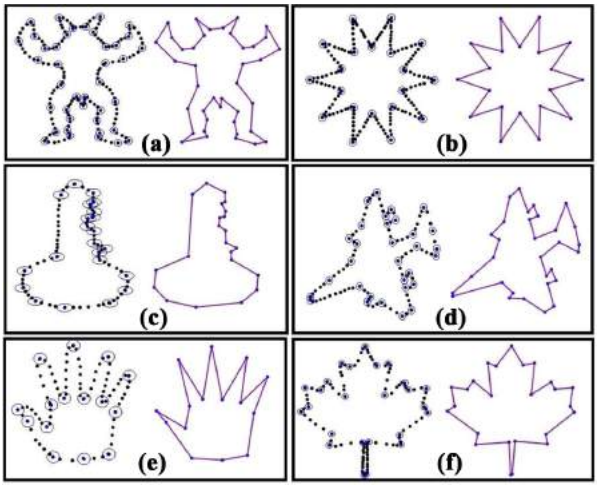

Figure 19: *Dominant points and the approximated polygons of various point sets. (a) armadillo (CR = 4.18), (b) star (CR = 8.65), (c) key (CR = 3.64), (d)aeroplane (CR = 3.26), (e) hand (CR = 5.73), and (f) leaf (CR = 4.52). Points in each set are ordered in counter-clockwise direction and the polygons are reconstructed by simply connecting these ordered points.*

differ in the construction of curves. While the shape-hull algorithm [PM15b] constructs curves by repeatedly eliminating boundary Delaunay triangles subjected to circumcentre and regularity properties, the proposed algorithm relies on an incremental Voronoi vertex labelling based on the spatial distribution of Voronoi vertices with respect to the original curve portions approximated by the tangent lines at point samples. Further, [PM15b] has been tuned only for reconstruction, whereas the algorithm presented in this paper can also extract MA as well as DPs. Compared to shape-hull, our algorithm nicely reconstructs divergent as well as non-divergent concave portions of closed curves as shown in Figure 10. Please note that the monkey point set has a non-divergent portion, which is well captured by our algorithm.

Table 1: *Statistical results of dominant point detection by different algorithms.*

Shape	Method	#DP	CR	ISE	FOM
Chromosome	[RR93]	18	3.33	5.57	0.6
($n = 60$)	[Wu03]	17	3.53	5.01	0.7
	Our method	21	2.85	25.35	0.1
Infinity	[RR93]	12	3.75	5.99	0.6
($n = 45$)	[Wu03]	13	3.46	5.17	0.7
	Our method	24	1.88	4.43	0.4

FOM values are truncated to one decimal place. A relatively high value of ISE for the chormosome is caused due to the lower pocket as highlighted in Figure 20.

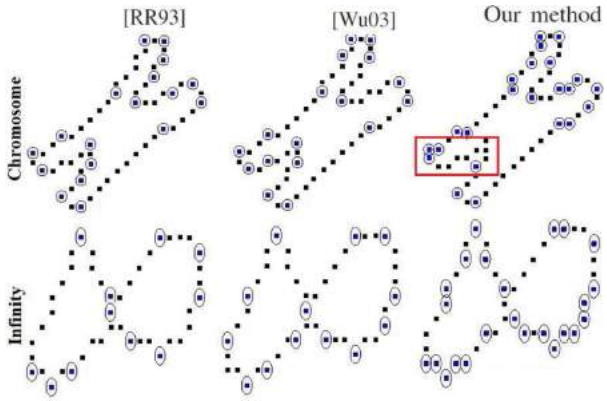

Figure 20: *Dominant points of benchmark data detected by various algorithms.*

Collection of curves. Our method also performs well in reconstructing a collection of closed curves from a sparsely sampled data as illustrated in the third row of Figure 9 and the top two rows in Figure 11. All the Voronoi vertices including a set of vertices between the samples of a pair of closed disconnected curves are classified as *outer* in the beginning of the algorithm. Incremental labelling on both the curves classifies the interior Voronoi vertices as *inner* and as a consequence, the proposed algorithm is able to separate the collection of curves.

Robustness to outliers. Most of the Delaunay/Voronoi-based algorithms interpolate the input data and hence found to be intolerant towards outliers. For point sets having noise and outliers, curve fitting techniques may be considered a more appropriate choice. Curve fitting techniques, however, make implicit assumptions on the underlying curve, which is highly impractical for sparse and non-uniform data. Since the incremental algorithm is also an interpolating technique, rather than eliminating the outliers from the results, we aim at showing the reconstruction of the original shape while retaining outliers in the scene. A post-processing step for denoising the output may be applied to eliminate outliers. Figure 11 (3–5 rows) visualizes a few more reconstruction results in the presence of outliers. The results clearly indicate the superiority of our algorithm in handling such inputs.

We experimented on a dove point set consisting of 54 points. Random outliers, expressed as a percentage of the point set size, were injected to the input data as shown in Figure 12. Our approach is noticeably better at dealing with the outliers constituting even 40% of the curve samples. Results by deGoes *et al.* [dGCSAD11] lose many fine details of the dove shape even for 10% outliers. However, a few artefacts appear in the reconstruction for 40% outliers in all the algorithms. The reconstruction by Parakkat and Muthuganapathy [PM16] and Parakkat *et al.* [PMM18] produces curve artefacts. Please note that, albeit the artefacts, dove shape has been well reconstructed by our method. This is mainly due to the label transition failures which occur when the incremental algorithm starts with EVVs induced fully or partially by the sparse outlier points. As a result, a continuous *inner* and *outer* combination of Voronoi vertices does not arise in the premise of outliers, thereby preventing them to be attached to the input curve.

Dealing with sharp corners. On closed and concave curves with sharp corners, our approach performs better than other methods. For instance, the left horn of oni which is sharp and pointed in Figure 13 is well captured by our algorithm as opposed to other crust algorithms. Though optimal transport-based approach reconstructs both the sharp corners well, it loses several other details such as neck of the oni. In contrast, our method not only captures the sharp corners but also preserves other details of the original curve. We would like to remark that a few works [DW02, Gie99, FR01] specially designed to work on sharp corners are expected to possibly capture the correct boundary of Oni data.

Figure 14 shows our results for point sets with sharp features. The incremental algorithm correctly reconstructs the shapes for point sets in Figures 14(a) and (b), for which all the TSP-based algorithms listed in [AMNS00] fail.

Quantitative analysis. We evaluate our algorithm quantitatively using L^2-error norm measure on the points sampled from the borders of various countries. L^2-error norm is the area of the symmetric difference between the original shape O and the reconstructed shape as a proportion of the total area of the original shape O [PM15a]. A zero value for L^2-error norm implies that the two shapes are equal in area and also their boundaries are aligned perfectly over each other. Figure 15 visualizes the symmetric difference (L^2-error) for the Luxemburg country shape with varying point densities. Figure 16 shows the L^2-error metric of various algorithms for varying point densities of different country shapes. Compared to the competitors, the proposed algorithm performed well for most of the country shapes. Please note that the test shapes were chosen based on the sinusoidal characteristics of the boundaries. A qualitative comparison of the performance of various algorithms with respect to the L^2-error metric on Zambia shape is presented in Figure 17. Compared to the other three methods in the figure, the proposed algorithm is very successful in capturing the concavities of the shape, even for the sparse input, as quantified in Figure 16(d).

Medial axis results: Figure 18 shows the reconstructed curves as well as the medial axes for various non-uniformly sampled data. Like any other approach, the approximation quality of our MA algorithm is limited by the sampling density of input data and the smoothness of the given curve. For a qualitative comparison, we have also presented the MAT results of local crust [Gol99] algorithm. For the given inputs, both the algorithms generated the same MATs. The results seem reasonable as both these algorithms perform MAT extraction on the underlying labelled Voronoi vertices; however, the labelling procedure differs considerably (see [Gol99] for details).

Dominant points of different data sets: Figure 19 shows the DPs (blue circles) and the approximated polygons of various point sets. Polygons are approximated from the DPs ordered along the original contour. Usually, polygonal approximation algorithms on digital curves are evaluated using metrics such as compression ratio ($\mathrm{CR} = \frac{\#inputpoints}{\#dominantpoints}$), integral square error (ISE), i.e. sum of squared distances of the curve points from approximating polygon or figure of merit ($\mathrm{FOM} = \frac{CR}{ISE}$). In our setting, which is mainly intended for extraction of shape structures from non-uniform points rather than digital curves, we resort to an evaluation based on qualitative analysis and the compression ratio.

The demonstrated results in Figure 19 indicate that the proposed framework is capable of detecting DPs at significant locations on the contours and consequently, generating polygons that preserve the morphology of the shape with a reasonable accuracy. However, for benchmark data such as chromosome and infinity, algorithms [RR93, Wu03] perform better than the proposed method in terms of FOM as shown in Table 1 and Figure 20. Our method still detects most of the DPs of these benchmarks. Our experimental study and comparison reveals that the proposed DP detection scheme is more suitable for non-uniformly sampled data with a high sampling rate along the high curvature portions of the contours as shown in Figure 19.

5. Conclusion

In this paper, we presented a multi-purpose Voronoi and Delaunay-based framework for curve reconstruction, MA approximation and DP detection. The key part of the framework is a simple incremental technique that classifies the Voronoi vertices into *outer* and *inner* with respect to the original curve. Under ϵ-sampling model, it has been established that the incremental algorithm constructs a piecewise linear approximation to smooth, closed and planar curves. Experimental results indicate that our approach is capable of reconstructing curves from sparse data. It also handles collection of curves successfully and captures sharp corners, though the algorithm is designed for smooth and closed curves. In the Delaunay/Voronoi-based domain, only algorithms such as conservative crust [DMR00] handle outliers, however, at the expense of parameter tuning. As opposed to this, our algorithm found to perform well in the case of curves with outliers without using any external parameter. In future, one can work on extending the framework for the reconstruction of multiply connected curves with a hierarchical incremental labelling.

Appendix

In the Appendix, we provide a few theoretical analyses and observations about the proposed algorithm. Primarily, we aim to prove that the reconstructed curve consists of only the edges between adjacent samples of $\mathcal{C}$. To argue for the correct reconstruction, we consider convex ($\mathcal{C}_{cvx}$) and concave ($\mathcal{C}_{ccv}$) portions separately.

Pseudo-convex portions: To achieve correct reconstruction of $\mathcal{C}_{cvx}$, all the finite Voronoi vertices, of infinite edges corresponding to the adjacent samples from $\mathcal{C}_{cvx}$, must lie interior to $Conv(P)$. We establish this claim in Lemma 5.1.

Lemma 5.1. *In $Vor(P)$, where P is ϵ-sampled from $\mathcal{C}$, EVVs of infinite edges between the adjacent samples of the pseudo-convex portions from $\mathcal{C}_{cvx}$ lie interior to $Conv(P)$.*

Proof. Consider two adjacent samples $p, q \in P$ from a pseudo-convex portion $C \in \mathcal{C}_{cvx}$ (refer to Figure A1) that lie at a maximum distance of $d(p,q) = \epsilon lfs(p)$. Let v be the finite Voronoi vertex of the infinite edge between p and q. We assume the contrary, i.e. v lies outside $Conv(P)$. Let $r \in P$ be a sample from $\mathcal{C}$ that induces v. As v lies outside $Conv(P)$, the sample r must be non-adjacent to either p or q along the curve. As v lies outside $Conv(P)$, it also lies outside the edge $(p,q) \in Conv(P)$ thereby making the $\triangle pqr$ obtuse at r. Consequently, $d(p,q) > d(p,r)$. This implies that a non-adjacent (along the curve) sample r lies within a sampling distance of $\epsilon lfs(s)$ for the sample p. This is a contradiction to the definition of ϵ-sampling and hence the lemma. □

Pseudo-concavities: The crucial part of the correctness proof lies in establishing the faithful reconstruction of pseudo-concavities. Each pseudo- concavity has a branch line consisting of EVV, middle SVVs and end SVVs as shown in Figure A2. Usually, a main branch line starts with an EVV and a sub-branch line starts with a middle SVV. A middle SVV can have either two or three adjacent outer Voronoi vertices. An end SVV is a Voronoi vertex whose two branching Voronoi edges are shared by three adjacent samples $p, q, r \in P$ from $\mathcal{C}$ (refer to Figure A3a).

We consider a curve Voronoi disc [ABE98] B of radius ϵ passing through two adjacent points $p, q \in P$ sampled from $\mathcal{C}$ (refer to Figure A3b). Without loss of generality, we assume the local feature

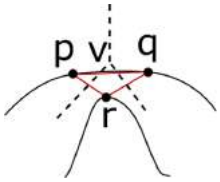

Figure A1: *(a) Illustration of Lemma 5.1.*

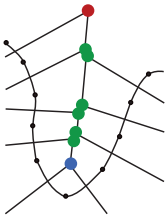

Figure A2: *Illustration of different SVVs in a pseudo-concavity. Red, green and blue dots represent EVV, middle SVVs and end SVV, respectively.*

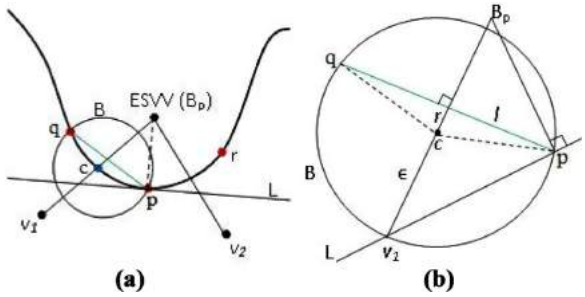

Figure A3: *(a) Construction for Lemma 5.2 and (b) a contradicting case for Lemma 5.2.*

size of the centre of B to be 1 ($lfs(c) = 1$). Due to Lemma 9 of [ABE98], we know that the angle formed by p and q at the curve Voronoi vertex c is $\pi - 2\arcsin\frac{\epsilon}{2}$. Let $B_p v_1$ is the bisector of the chord qp. From Figure A3(b), it is easy to verify the following:

1. $l = \frac{\epsilon}{2}\sqrt{4-\epsilon^2}$
2. $r = \frac{\epsilon^2}{2}$
3. $\angle qcv_1 = \frac{\pi}{2} + \arcsin(\frac{\epsilon}{2})$
4. $\angle qpv_1 = \arctan(\frac{2+\epsilon}{\sqrt{4-\epsilon^2}})$

Next, few lemmas have been proved under the assumption that the Voronoi cell V_p is a part of VD induced by a set of points ϵ-sampled from $\mathcal{C}$.

Lemma 5.2. *End SVV and the other Voronoi vertices of V_p lie on either side of the line L perpendicular to $\overline{B_p, p}$ for $\epsilon \leq 0.4$.*

Proof. In theorem 14 of [ABE98], Amenta *et al.* showed that curve Voronoi discs [ABE98] do not contain any vertices of $Vor(P)$ for $\epsilon \leq 0.4$. We adapt their theorem to our algorithmic conditions and establish the lemma (refer to Figure A3 for an illustration). Consider three adjacent samples p, q, r from a pseudo-concavity of $\mathcal{C}_{ccv}$ that induce an end source vertex B_p. Let $e_1 = (B_p, v_1)$ and $e_2 = (B_p, v_2)$ are the Voronoi bisectors of p, q and p, r, respectively. Let B be a curve Voronoi disc passing through samples p and q, which is centred at the curve Voronoi vertex [ABE98] c. We show that B_p and v_1 lie on either side of L, where L is the line passing through p orthogonal to $\overline{B_p q}$.

Theorem 14 of [ABE98] implies that v_1 can move only along the boundary or outside of B. Assume the case where v_1 approaches the sample p along the boundary of B. v_1 crosses L only after coinciding with the sample p, during which, the line e_1 becomes a non-bisector of p and q. This contradicts our assumption on e_1.

Similarly, consider the case where v_1 approaches the sample q along the boundary of B. Suppose, it coincides with the point of intersection of L with ∂B on its way as shown in Figure A3(b). The angle subtended by the chord qv_1 at the point p must be half the central angle ($\angle qcv_1$) subtended by it, i.e. $\angle qpv_1 = \frac{1}{2}\angle qcv_1$.

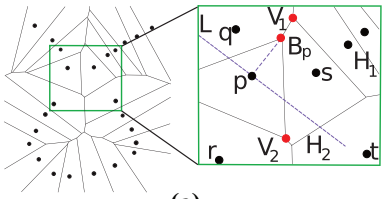

(a)

Figure A4: *Illustration showing the existence of active Voronoi vertices in pseudo-concavities.*

On substituting the values for r and l from Figure A3(b), we get Equation (A.1):

$$\arctan\left(\frac{2+\epsilon}{\sqrt{4-\epsilon^2}}\right) = \frac{1}{2}\left(\frac{\pi}{2} + \arcsin\left(\frac{\epsilon}{2}\right)\right). \qquad \text{(A.1)}$$

We can observe that Equation (A.1) does not hold for any values of ϵ in the interval $[0, 1]$ (consequently for $\epsilon \in [0, 0.4]$). Hence, vertex v_1 cannot merge with the point of intersection of L and ∂B on its way to q. Further, it cannot move nearer to q as it violates the assumption that it orthogonally bisects the chord pq of B. Hence, v_1 can lie only on or outside ∂B in the half plane opposite to the one that containing B_p. Similar arguments hold for the vertex v_2 as well and hence the lemma. □

To show the existence of outer Voronoi vertices in pseudo-concavities, we consider the construction in the inset of Figure A4. It consists of five samples three of which q, p, r are adjacent, Voronoi cell V_p of a sample $p \in P$, its SVV (B_p) and Voronoi vertices v_1 and v_2 adjacent to B_p lying in the pseudo- concave region. The samples s, t are adjacent to each other and non-adjacent to p, q, r. Let L be the line orthogonal to $\overline{B_p p}$. We need to show that v_2 lies in the half plane containing B_p with respect to L. It is obvious from Figure A4 that v_2 is either induced by $\triangle psr$ or $\triangle pst$. For the sake of argument, we assume that v_2 is a Voronoi vertex induced by samples p, s and r.

Since we need the half planes to be unchanging, we will fix the samples q, p, s and analyse the effect of the location of v_2 on r. As v_2 moves away from L in H_2, r also tends to move apart from the samples p and s. This will ultimately cause a violation on ϵ-sampling as it is evident that $d(p, r)$ will be greater than $d(p, s)$ and s is a non-adjacent sample of p. So, under a sufficiently dense sampling, v_2 always tends to lie on or away from L in H_1. A similar argument holds good if we consider that v_2 is induced by $\triangle pst$.

Proposition 5.3. *The curve reconstructed by the incremental algorithm for a finite set of points P, where P is ϵ-sampled from a smooth, closed and planar curve $\mathcal{C}$, contains an edge between every pair of adjacent samples of $\mathcal{C}$, for $\epsilon < 0.4$.*

Proof. We argue for the piece-wise linear reconstruction of $\mathcal{C}_{cvx}$ and $\mathcal{C}_{ccv}$. Due to Lemma 5.1, all the finite Voronoi vertices on the infinite edges corresponding to adjacent samples from $\mathcal{C}_{cvx}$ are labelled outer and subsequently the algorithm constructs a piece-wise linear approximation to $\mathcal{C}_{cvx}$. We know that there exists at least one finite Voronoi vertex corresponding to each pseudo-concavity outside $Conv(P)$ (Lemma 3.1) and hence the labelling happens for each pseudo-concavity of $\mathcal{C}$. Lemma 5.2 ensures that the edges between the adjacent samples in the pseudo-concavities have outer and inner Voronoi vertices. Further, it ensures that the labelling does not get into the interior of $\mathcal{C}$. Finally, existence of a proper branch line that covers the entire pseudo-concavity is captured in Figure A4. We conclude that under sufficiently dense sampling, the reconstructed curve represents a piece-wise linear approximation to $\mathcal{C}$, where $\mathcal{C}$ is a smooth, closed planar curve. □

Medial axis: As a consequence of Proposition 5.3, the curve reconstructed by the proposed algorithm represents a piece-wise linear representation to $\mathcal{C}$. All the inner Voronoi vertices represent the centres of the interior Voronoi discs. In [GMP07b], the authors established that the MA of $\mathcal{C}$ can be approximated from the centres of the interior Voronoi discs of $Vor(P)$, where P is ϵ-sampled from $\mathcal{C}$ for certain $\epsilon < 0.207$. Since MAT is an approximation from the centres of interior Voronoi discs, the theory is equally applicable to our MA approximation for concave and closed curves.

References

[AB98] Amenta N., Bern M.: Surface reconstruction by Voronoi filtering. In *Proceedings of the 14th Annual Symposium on Computational Geometry* (New York, NY, USA, 1998), SCG '98, ACM, pp. 39–48.

[ABE98] Amenta N., Bern M., Eppstein D.: The crust and the beta-skeleton: Combinatorial curve reconstruction. *Graphical Models and Image Processing 60*, 2 (1998), 125–135.

[ACK01] Amenta N., Choi S., Kolluri R. K.: The power crust, unions of balls, and the medial axis transform. *Computational Geometry 19*, 2–3 (2001), 127–153.

[AK01] Amenta N., Kolluri R. K.: The medial axis of a union of balls. *Computational Geometry 20*, 1–2 (2001), 25–37.

[AM97] Attali D., Montanvert A.: Computing and simplifying 2D and 3D continuous skeletons. *Computer Vision and Image Understanding 67*, 3 (1997), 261–273.

[AM01] Althaus E., Mehlhorn K.: Traveling salesman-based curve reconstruction in polynomial time. *SIAM Journal on Computing 31*, 1 (2001), 27–66.

[AMNS00] Althaus E., Mehlohrn K., Naher S., Schirra S.: Experiments on curve reconstruction. In *Proceedings of 2nd Workshop on Algorithms Engineering Experiments* (2000), pp. 104–114.

[Att54] Attneave F.: Some informational aspects of visual perception. *Psychological Review 61*, 3 (May1954), 183–193.

[Att98] Attali D.: r-regular shape reconstruction from unorganized points. *Computational Geometry 10*, 4 (1998), 239–247.

[BA92] Brandt J. W., Algazi V.: Continuous skeleton computation by Voronoi diagram. *CVGIP: Image Understanding 55*, 3 (1992), 329–338.

[Bra94] Brandt J.: Convergence and continuity criteria for discrete approximations of the continuous planar skeleton. *CVGIP: Image Understanding 59*, 1 (1994), 116–124.

[CFG*05] Cheng S.-W., Funke S., Golin M., Kumar P., Poon S.-H., Ramos E.: Curve reconstruction from noisy samples. *Computational Geometry 31*, 1–2 (2005), 63–100.

[dGCSAD11] de Goes F., Cohen-Steiner D., Alliez P., Desbrun M.: An optimal transport approach to robust reconstruction and simplification of 2D shapes. *Computer Graphics Forum 30*, 5 (2011), 1593–1602.

[DK99] Dey T. K., Kumar P.: A simple provable algorithm for curve reconstruction. In *Proceedings of the 10th Annual ACM-SIAM Symposium on Discrete Algorithms* (1999), SODA '99, pp. 893–894.

[DMR00] Dey T. K., Mehlhorn K., Ramos E. A.: Curve reconstruction: Connecting dots with good reason. *Computational Geometry 15*, 4 (2000), 229–244.

[Dun86] Dunham J. G.: Optimum uniform piecewise linear approximation of planar curves. *IEEE Transactions on Pattern Analysis and Machine Intelligence 8*, 1 (1986), 67–75.

[DW01] Dey T. K., Wenger R.: Reconstructing curves with sharp corners. *Computational Geometry 19*, 2–3 (2001), 89–99.

[DW02] Dey T. K., Wenger R.: Fast reconstruction of curves with sharp corners. *International Journal of Computational Geometry & Applications 12*, 05 (2002), 353–400.

[EKS83] Edelsbrunner H., Kirkpatrick D., Seidel R.: On the shape of a set of points in the plane. *IEEE Transactions on Information Theory 29*, 4 (July1983), 551–559.

[FEC02] Fabbri R., Estrozi L. F., Costa L. F.: On Voronoi diagrams and medial axes. *Journal of Mathematical Imaging and Vision 17*, (2002), 27–40.

[FR01] Funke S., Ramos E. A.: Reconstructing a collection of curves with corners and endpoints. In *Proceedings of the 12th Annual ACM-SIAM Symposium on Discrete Algorithms* (2001), SODA '01, pp. 344–353.

[GDN04] Guru D., Dinesh R., Nagabhushan P.: Boundary based corner detection and localization using new 'cornerity' index: A robust approach. In *Proceedings of the 1st Canadian Conference on Computer and Robot Vision, 2004* (May 2004), pp. 417–423.

[Gie99] Giesen J.: Curve reconstruction, the traveling salesman problem and Menger's theorem on length. In *Proceedings of the 15th Annual Symposium on Computational Geometry* (New York, NY, USA, 1999), SCG '99, ACM, pp. 207–216.

[GMP07a] Giesen J., Miklos B., Pauly M.: Medial axis approximation of planar shapes from union of balls: A simpler and more robust algorithm. In *proceedings of Canadian Conference of Computational Geometry (CCCG)* (Ottawa, Canada, 2007), P. Bose (Ed.), pp. 105–108.

[GMP07b] Giesen J., Miklos B., Pauly M.: Medial axis approximation of planar shapes from union of balls: A simpler and more robust algorithm. In *Proceedings of the 19th Annual Canadian Conference on Computational Geometry, CCCG 2007, August 20–22, 2007, Carleton University, Ottawa, Canada* (2007), pp. 105–108.

[Gol99] Gold C.: Crust and anti-crust: A one-step boundary and skeleton extraction algorithm. In *Proceedings of the 15th Annual Symposium on Computational Geometry* (New York, NY, USA, 1999), SCG '99, ACM, pp. 189–196.

[HAA94] Held A., Abe K., Arcelli C.: Towards a hierarchical contour description via dominant point detection. *IEEE Transactions on Systems, Man and Cybernetics 24*, 6 (June 1994), 942–949.

[HS99] Huang S.-C., Sun Y.-N.: Polygonal approximation using genetic algorithms. *Pattern Recognition 32*, 8 (1999), 1409–1420.

[KD82] Kurozumi Y., Davis W. A.: Polygonal approximation by the minimax method. *Computer Graphics and Image Processing 19*, 3 (1982), 248–264.

[Lee00] Lee I.-K.: Curve reconstruction from unorganized points. *Computer Aided Geometric Design 17*, 2 (2000), 161–177.

[LWS*15] Li P., Wang B., Sun F., Guo X., Zhang C., Wang W.: Q-mat: Computing medial axis transform by quadratic error minimization. *ACM Transactions on Graphics 35*, 1 (December 2015), 8:1–8:16.

[Mas08] Masood A.: Optimized polygonal approximation by dominant point deletion. *Pattern Recognition 41*, 1 (2008), 227–239.

[MBS16] M. Berger Andrea Tagliasacchi L. S. P. A. G. G. J. L. A. S., Silva C.: A survey of surface reconstruction from point clouds. *Computer Graphics Forum'16 (extended journal version of the EG STAR) 36*, (2016), 301–329.

[MGP07] Miklos B., Giesen J., Pauly M.: Medial axis approximation from inner Voronoi balls: A demo of the Mesecina tool. In *Proceedings of the 23rd Annual Symposium on Computational Geometry* (New York, NY, USA, 2007), SCG '07, ACM, pp. 123–124.

[MPM15] Methirumangalath S., Parakkat A. D., Muthuganapathy R.: A unified approach towards reconstruction of a planar point set. *Computer Graphics 51* C (October 2015), 90–97.

[MS03] Marji M., Siy P.: A new algorithm for dominant points detection and polygonization of digital curves. *Pattern Recognition 36*, 10 (2003), 2239–2251.

[OM13] Ohrhallinger S., Mudur S. P.: An efficient algorithm for determining an aesthetic shape connecting unorganized 2D points. *Computer Graphics Forum 32*, 8 (2013), 72–88.

[OMW16] Ohrhallinger S., Mitchell S., Wimmer M.: Curve reconstruction with many fewer samples. *Computer Graphics Forum 35*, 5 (2016), 167–176.

[O'R98] O' Rourke J.: *Computational Geometry in C*, 2nd ed. Cambridge University Press, New York, 1998.

[OW18] Ohrhallinger S., Wimmer M.: Fitconnect: Connecting noisy 2D samples by fitted neighborhoods. *Computer Graphics Forum*, Early view (April 2018) https://doi.org/10.1111/cgf.13395.

[PM15a] Peethambaran J., Muthuganapathy R.: A non-parametric approach to shape reconstruction from planar point sets through Delaunay filtering. *Computer-Aided Design 62* (2015), 164–175.

[PM15b] Peethambaran J., Muthuganapathy R.: Reconstruction of water-tight surfaces through Delaunay sculpting. *Computer-Aided Design 58*, 0 (2015), 62–72.

[PM16] Parakkat A. D., Muthuganapathy R.: Crawl through neighbors: A simple curve reconstruction algorithm. *Computer Graphics Forum 35*, 5 (2016), 177–186.

[PMM18] Parakkat A. D., Methirumangalath S., Muthuganapathy R.: Peeling the longest: A simple generalized curve reconstruction algorithm. *Computers & Graphics 74*, (2018), 191–201.

[PNK98] Pal N. R., Nandi S., Kundu M. K.: Self-crossover-A new genetic operator and its application to feature selection. *International Journal Systems of Science 29*, 2 (1998), 207–212.

[PPM15] Peethambaran J., Parakkat A., Muthuganapathy R.: A Voronoi based labeling approach to curve reconstruction and medial axis approximation. In *Pacific Graphics 2015* (October 2015), Eurographics Digital Library.

[Ram72] Ramer U.: An iterative procedure for the polygonal approximation of plane curves. *Computer Graphics and Image Processing 1*, 3 (1972), 244–256.

[RR93] Ray B. K., Ray K. S.: Determination of optimal polygon from digital curve using {L1} norm. *Pattern Recognition 26*, 4 (1993), 505–509.

[Sat92] Sato Y.: Piecewise linear approximation of plane curves by perimeter optimization. *Pattern Recognition 25*, 12 (1992), 1535–1543.

[TC89] Teh C.-H., Chin R.: On the detection of dominant points on digital curves. *IEEE Transactions on Pattern Analysis and Machine Intelligence 11*, 8 (August 1989), 859–872.

[TDS*16] Tagliasacchi A., Delame T., Spagnuolo M., Amenta N., Telea A.: 3D skeletons: A state-of-the-art report. *Computer Graphics Forum (Proceedings of Eurographics) 35*, (2016), 573–597.

[Wan14] Jun W., Zeyun Y., Weizhong Z., Mingqiang W., Changbai T., Ning D., Xi Z.: Robust reconstruction of 2D curves from scattered noisy point data. *Computer-Aided Design 50*, 0 (2014), 27–40.

[Wu02] Wu W.-Y.: A dynamic method for dominant point detection. *Graphical Models 64*, 5 (2002), 304–315.

[Wu03] Wu W.-Y.: An adaptive method for detecting dominant points. *Pattern Recognition 36*, 10 (2003), 2231–2237.

[YIN99] YIN P.-Y.: Genetic algorithms for polygonal approximation of digital curves. *International Journal of Pattern Recognition and Artificial Intelligence 13*, 07 (1999), 1061–1082.

[ZC18] Zhong Y., Chen F.: Computing medial axis transformations of 2D point clouds. *Graphical Models 97*, (2018), 50–63.

[ZSC*14] Zhu Y., Sun F., Choi Y.-K., Jüttler B., Wang W.: Computing a compact spline representation of the medial axis transform of a 2D shape. *Graphical Models 76*, 5 (2014), 252–262.